JOM, Vol. 66, No. 10, 2014
DOI: 10.1007/s11837-014-1124-7

Bulk-Forming Simulation of Bimetallic Watchcase Components

T.F. KONG[1,2] and L.C. CHAN[1,3]

1.—Department of Industrial and Systems Engineering, The Hong Kong Polytechnic University, Hung Hom, Kowloon, Hong Kong, China. 2.—e-mail: tf.kong@polyu.edu.hk. 3.—e-mail: lc.chan@polyu.edu.hk

This article presents a study of the effects of process parameters in bulk-forming bimetallic watchcase components using finite-element (FE) simulation. This study aimed to determine the suitable forming temperature T and ram speed S for attaining the complete die filling of bimetals. A complicated watchcase component made of 3-mm-thick AISI 316L stainless steel (SS316L) and 6-mm-thick 6063 aluminum alloy (AA6063) was used as the example. The processes were simulated with T of 400°C, 500°C, 600°C, 700°C, 800°C, and 900°C and S of 20 mm/s, 40 mm/s, and 60 mm/s. Although the AA6063 was not heated in the beginning, it flowed faster than the SS316L during the process, and hence, the incomplete die filling was found mainly in the SS316L region. To avoid the incomplete die filling and strengthen the intermetallic bond between two dissimilar metals, the T of 900°C was suggested. The S of 40 mm/s was recommended also because this could save much forming energy and prevent the damage of tools. The experimental verification was carried out under process conditions that were employed in the simulations. An infrared thermal imaging camera and a 300-ton mechanical press were used to monitor the T and testify the bulk-forming operation, respectively. The data acquired from the experiments, on average, agreed strongly with those predicted by the simulations. On the basis of the results in this study, engineers can gain a better understanding of bulk-forming bimetallic components and be able to determine the T and S efficiently for similar processes.

INTRODUCTION

Bulk forming is an efficient manufacturing process. In this process, a bulk workpiece (with a small area-to-volume ratio) such as a block, a billet, and a preform is deformed permanently to the desired shape without damage to its material structure. Due to its high productivity and the advantage of material-strength improvement, it is used commonly in automobile and machinery manufacturing. Groche and Fritsche,[1] Groche et al.,[2] and Behrens et al.[3] convincingly demonstrated the production of mechanical components by flow forming, incremental bulk metal forming, and precision forging, respectively; they are classified into bulk-forming processes to achieve high plastic strains on a workpiece.

Nowadays the market trend of the bulk-forming industry is toward demands on light, strong, and economical metalwork. In fact each material has its unique properties and characteristics, and hence, no single metal or alloy can fully meet the above requirements. For example, titanium and aluminum are lighter than alloy steel for making the armor of tanks. However, the titanium is costly while the aluminum does not have sufficient strength and wear resistance. The use of bimetal is an alternative in which two different metals or alloys are joined together to take advantage of their usefulness and cost-effectiveness. Sapozhnikov et al.[4] showed that the use of bimetals (medium-carbon and low-alloy steels cladded with a bronze layer) could save up to 80% cost for making hydraulic pumps with an acceptable performance. Taylor and Pan[5] presented a tapered steel stud and aluminum knuckle assembly for weight reduction in automobiles. Yilmaz and Çelik[6] found that the thermal conductivities of interfaces of diffusion bonded and soldered bimetals (copper and stainless steel) could be affected by their joining parameters, and thus, they could be used for particular electrical applications. Şimşir et al.[7] used the shell mold casting technique to fabricate a bimetal

(Published online September 4, 2014)

(316L grade stainless steel and structural steel with 30CrNiMo8). The tensile strength and yield strength of this bimetal was higher than those of the stainless steel. Torbati et al.[8] investigated the optimization procedures for autogenous gas tungsten arc welding of bimetals (duplex stainless steel pipe) that had a notable achievement in cost reduction, and improvement of corrosion and fatigue resistance.

Both heat and pressure are important in bulk-forming bimetallic components. The sufficient heat energy and plasticity (i.e., plastic deformation) are not only used for shaping the components, but also they are necessary to generate the intermetallic bond between two dissimilar metals as known as solid-state welding. Yildirim and Kelestemur[9] joined the boron-doped Ni_3Al intermetallic compound with AISI 304 stainless steel by solid-state welding such that an acceptable residual stress was found in the weld interface. Zhang et al.[10] investigated the feasibility of isothermal superplastic solid-state welding of 40Cr steel and QCr0.5, ZQSn6-6-3 copper alloys, the deformation of copper alloys occurred during the welding process, and the deformation of 40Cr steel was restricted. Kahraman et al.[11] and Akbari Mousavi and Farhadi Sartangi[12] demonstrated that the explosive welding could join the CP-titanium and austenitic stainless steel through impact energy and pressure. The grains in the weld interface were elongated because the plastic deformation occurred in the explosion. Nevertheless, since the flow properties and mechanical behaviors of each material are different, the study of bulk-forming bimetallic components is more complicated than that of single metal components, particularly in the prediction of such material flow.

Many factors can influence the material flow as well as the die-filling in the bulk-forming process. They include forming temperatures, ram speeds, tool geometries, workpiece geometries, frictional conditions at tool/material interfaces, *etc*.[13] Therefore, Neugebauera et al.[14] and Osakada et al.[15] had fully explained the importance of both velocity (or strain rate) effects and ram speed of mechanical presses in various metal-forming processes. Groche et al.[16] and Manuel et al.[17] studied the surface roughness and nonfriction conditions between the tool and workpiece interface in cold-forging processes. Interactions of these factors often create difficulties in finding exact mathematical solutions to the real phenomenon occurring in the bulk-forming process. For this reason, finite-element (FE) simulation has been developed, which can effectively and rapidly predict the complicated material flow with various process parameters, and hence, the cost and time spent on practical trials can be reduced greatly. Ahmad and Groche[18] also developed the algorithms for speeding up the FE simulation of incremental bulk forming.

Most previous investigations in bulk-forming bimetallic components have focused mainly on cold forming, especially cold extrusion for rods[19–21] and tubes[22–24] as well as cold rolling for strips.[25,26] Even though Raßbach and Lehnert[27] studied warm-upsetting of bimetals, their study was carried out at a constant temperature and the changes of temperature of the workpieces were not considered. In fact, the influence of changing temperature on material flow is very significant in bulk-forming bimetallic components at an elevated temperature. However, very little literature has been published on this topic and the available information about it is minimal.

This article presents a study of the effects of process parameters in bulk-forming, bimetallic, non-axisymmetric watchcase components at elevated temperatures using FE simulation. This study aimed to determine the suitable forming temperature T and ram speed S for attaining the complete die filling of bimetals. A complicated non-axisymmetric watchcase made of AISI 316L stainless steel (SS316L) and 6063 aluminum alloy (AA6063) was chosen as the example. A comprehensive analysis of material flow was carried out at different T and S. Corresponding experimental tests during this study included the production of a series of bimetallic components. The specimens were heated by an induction coil, and the T was monitored by an advanced infrared thermal imaging camera. A 300-ton mechanical press operating at different S could form the specimens into the required shape. These experiments both verified the proposed methodology and the simulation results.

BIMETALLIC WATCHCASE COMPONENT

The bimetallic watchcase component demonstrated in this study was a non-axisymmetric component. Figure 1 shows its configurations and detailed dimensions. Compared with most conventional axisymmetric-formed components, such as automotive break discs, valve heads, and wheel hubs, and other non-axisymmetric components, the shape complexity of this component was much greater (surface-to-volume ratio = 0.53), which increased the difficulty for manufacturing as well as for the determination of process parameters. Therefore, it was especially preferable as a typical example, which would provide useful information about the bulk-forming of such intricate bimetallic components. The scientific conclusion drawn through the analysis of both simulations and experimental results could also be generalized and applied to the forming of other bimetallic circular or axisymmetric components.

The present component could be produced by the closed-die forging process in one stroke. Parting lines of the die were placed at the area with the largest cross section, center hole, and around the entire perimeters that were based partially on the gain-flow considerations. Flashes were extruded accordingly at the parting lines after the die cavity had been filled completely. To reduce the scrap rate, the external flash thickness was minimized to

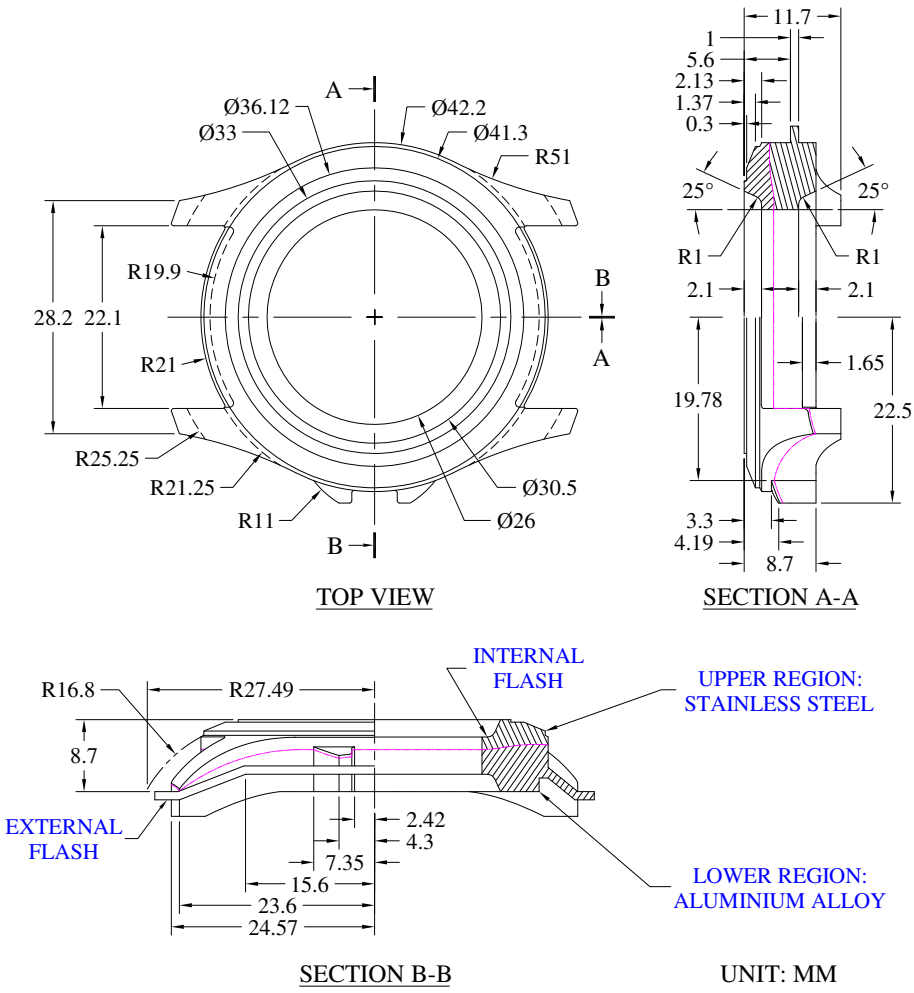

Fig. 1. The final shape of a bimetallic watchcase component used as an example in this study.

1.0 mm. Indeed the flash thickness is an important factor influencing the die filling and forming load. The flash land on the die becomes smaller by decreasing the flash thickness that leads to the restriction of metal flow and increases the frictional forces. Since metal always flows along the path with the least resistance, the die cavity should be filled before the excess material is extruded to the smaller flash land. A larger forming load is also required to compress the metal into the thinner flash. The influence of flash thickness is expected and understood reasonably well from a qualitative viewpoint; hence, the analysis of flash thickness on the die filling and forming load has been excluded from this study.

The upper region and the lower region of the component were made of 3-mm-thick SS316L and 6-mm-thickness AA6063, respectively. In other words, the lower preform was the SS316L and the upper preform was the AA6063. Figure 2 is the design of the bimetallic hollow preforms. The component was hollow having a center hole. The preforms were constructed accordingly as the hollow shapes to reduce the forming load greatly.[28] An identical outer profile along the thickness of the preforms was shrunk by 0.2 mm from the outer profile of the component. This led the preforms that could be fitted properly inside the cavity of lower die as shown in Fig. 3. The volume of the component with expected flashes was approximately 8380 mm^3. While the whole component was made of SS316L, the weight was around 66.2 g. In this example, nearly 66.3% of volume of the component was made of AA6063. The weight of the component could be reduced to 37.3 g with around 43.6% of weight reduction, while the SS316L upper region could provide better wear resistance as well. This was a good applicable instance to reveal the benefits and advantages of using bimetals in metalwork.

The SS316L and AA6063 are dissimilar metals containing distinctive chemical compositions as given in Table I. There was no doubt about their weldability since previous researchers[29–32] had reported that such combinations of dissimilar metals could be joined by solid-state welding. If two metals are welded successfully, a narrow diffusion

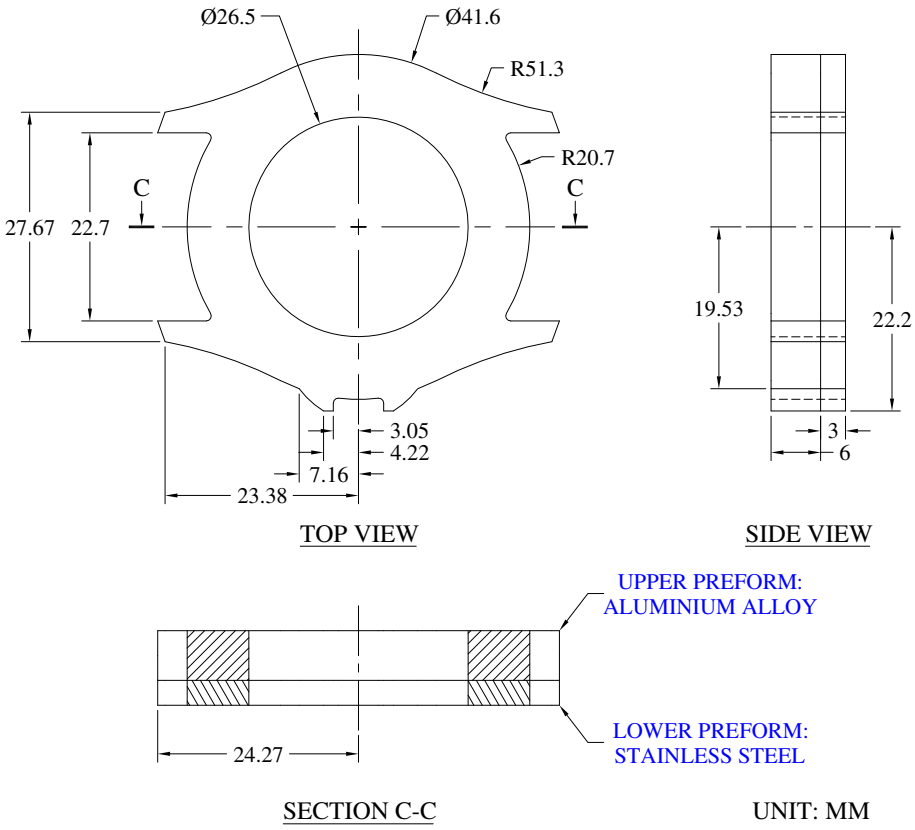

Fig. 2. The proposed design of the bimetallic hollow preforms.

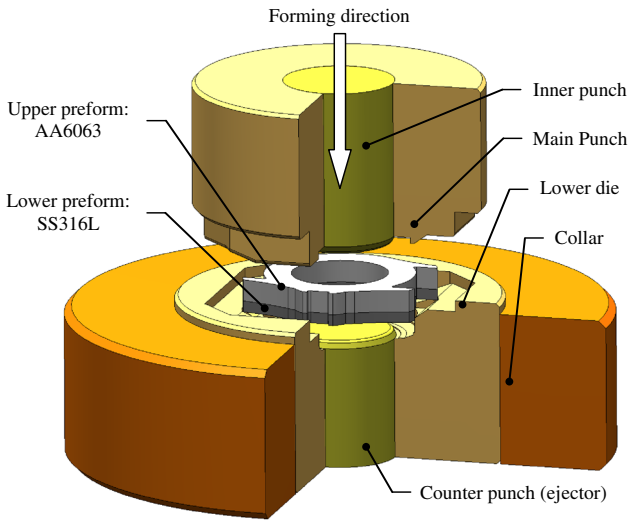

Fig. 3. A schematic diagram for the setup of tooling and preforms required to bulk form the component.

layer (i.e., intermetallic layer) can be found at the joint interface. This layer typically consisted of the intermetallic compounds of iron (Fe) and aluminum (Al) such as $FeAl_3$, Fe_2Al_5, Fe_3Al, AlFe, Al_5Fe_2, and $Al_{13}Fe_4$, and the joint efficiency could be nearly 100%.

On the other hand, the flow properties of SS316L and AA6063 are extremely different. Tables II and III are the flow stress data of SS316L at temperatures of 20°C, 400°C, 600°C, 700°C, 800°C, 900°C, 1000°C, and 1100°C and strain rates of 0.1 s^{-1}, and 1 s^{-1} and AA6063 at temperatures of 20°C, 100°C, 200°C, 300°C, 400°C, and 500 °C and strain rates of 0.1 s^{-1}, and 1 s^{-1}, respectively.[33–35] These flow stress data and the thermal properties[36] listed in Table IV were employed for modeling the rigid-viscoplastic materials in the simulation.

PROCESS MODELING

A series of bimetal bulk-forming process simulations was modeled using the commercial FE-simulation software DEFORM-3D. The program was able to perform the non-isothermal three-dimensional rigid-plastic/viscoplastic analysis of massive deformation. The von-Mises flow criterion was employed. The models for the bimetallic system were created by two separated rigid-viscoplastic objects with respective material behavior according to the flow properties and thermal properties given in Tables II, III, IV, and V. A penalty-based contact constraint and an average 0.5 shear friction factor were added between those two specimen materials. The friction factor was obtained by both physical experiment and simulation of ring-compression tests at a dry friction condition. All tool components were assumed as rigid-body objects. To improve the accuracy of material-flow prediction,

Table I. Chemical compositions of specimen materials: SS316L and AA6063

	Chemical composition (wt.%)													
Material	**Cr**	**Mn**	**Si**	**Fe**	**Mo**	**Ni**	**P**	**S**	**C**	**Al**	**Cu**	**Mg**	**Ti**	**W**
SS316L	16	1.7	0.5	Bal.	2.1	10	0.03	0.02	0.02	–	–	–	–	–
AA6063	0.1	0.1	0.4	0.3	–	–	–	–	–	Bal.	0.08	0.5	0.08	0.1

Table II. Flow stress data of SS316L[34,35]

Strain rate (s^{-1})	True strain	True stress (MPa)							
		20°C	**400°C**	**600°C**	**700°C**	**800°C**	**900°C**	**1000°C**	**1100 °C**
0.1	0.1	650.0	530.0	389.6	360.4	352.0	244.9	157.8	109.9
0.1	0.2	790.0	610.0	511.2	443.9	383.4	261.3	171.5	120.1
0.1	0.3	880.0	655.0	560.8	485.4	385.6	269.4	175.8	121.6
0.1	0.4	970.0	700.0	592.4	509.1	405.2	271.8	175.9	119.9
0.1	0.5	980.0	715.0	625.8	535.6	420.0	283.7	176.4	117.6
1	0.1	675.0	532.5	389.4	363.2	324.5	280.2	198.5	136.3
1	0.2	815.0	612.5	506.0	445.3	391.3	314.8	219.5	143.1
1	0.3	900.0	657.5	549.9	488.0	419.6	328.4	228.9	147.2
1	0.4	985.0	702.5	572.7	498.8	427.8	324.8	228.4	146.3
1	0.5	990.0	717.5	588.3	511.2	435.4	327.3	226.9	141.3

Table III. Flow stress data of AA6063[34,35]

Strain rate (s^{-1})	True strain	True stress (MPa)					
		20°C	**100°C**	**200°C**	**300°C**	**400°C**	**500°C**
0.1	0.1	215.3	206.1	187.7	169.3	56.2	32.1
0.1	0.2	218.6	209.4	191.0	172.6	58.1	32.9
0.1	0.3	224.4	215.3	197.1	178.9	60.6	33.6
0.1	0.4	222.9	214.2	196.8	179.4	61.3	33.9
0.1	0.5	221.3	212.9	196.1	179.3	62.3	34.0
1	0.1	296.0	287.7	271.1	254.5	77.0	45.9
1	0.2	308.6	299.2	280.4	261.6	80.4	47.3
1	0.3	308.8	299.0	279.4	259.8	83.5	48.0
1	0.4	308.7	298.7	278.7	258.7	84.2	48.0
1	0.5	305.4	295.4	275.4	255.4	85.1	47.7

Table IV. Thermal properties of SS316L and AA6063[36]

Material	**Thermal conductivity (W/m·K)**	**Heat capacity (J/g·K)**	**Emissivity**
SS316L	21.4	0.65	0.35
AA6063	180.2	0.24	0.35

all geometric models had been halved so as to speed up computations and increase the number of tetrahedral meshes for each volume.

During the bimetal bulk-forming process, the discrepancy of flow stress of two different materials might cause the heterogeneous material flow, which should be minimized by the control of process parameters. At the same strain rates, the flow stress of SS316L, at 900–1100°C, was close to that of AA6063 at 20–300°C. It was supposed that the heat transfer occurred at the contact surface between the two specimen materials. Hence, in this study, the simulations were conducted with T (the forming temperatures of SS316L) of 400°C, 500°C, 600°C,

Table V. Summary of the process conditions for simulation

Simulation parameter	Value/setting
Number of elements of SS316L	10850
Number of elements of AA6063	38855
Thickness of SS316L preform (mm)	3
Thickness of AA6063 preform (mm)	6
Iteration method	Direct method
Deformation solver	Sparse
Temperature solver	Sparse
SS316L/AA6063 shear friction factor	0.5
Preform/tool shear friction factor	0.25
Heat-transfer coefficient between each object (MW/m^2 K)	11
Forming stroke (mm)	11
Temperature of main punch and inner punch (°C)	20
Temperature of lower die and ejector (°C)	280
Forming temperature of SS316L (°C)	400/500/600/700/800/900
Forming temperature of AA6063 (°C)	20
Ram speed (mm/s)	20/40/60

700°C, 800°C, and 900°C and S of 20 mm/s, 40 mm/s, and 70 mm/s when the temperature of AA6063 was 20°C. Table V is the summary of the simulation conditions.

Corresponding simulations were run to their conclusions. The die-filling analysis at the end of forming stroke was based on the minimum distance between the formed component and the die cavity, which could be measured in the postprocessor of DEFORM-3D. The die-filling completion as well as the predicted forming loads of each trial were compared with those of the actual experiments as direct verification.

EXPERIMENTAL WORK

The experimental verification was carried out using a 300-ton mechanical press. The ram speeds of average 20 mm/s, 40 mm/s, and 60 mm/s could be achieved (these are the average values within the effective forming stroke) by interchanging the belt and pulley system that were connected to the motor and flywheel of the machine. A radio-frequency (RF) power supply and an induction coil were used to heat the SS316L preforms up to the test temperatures. The T were then monitored by an infrared thermal imaging camera during the first instant of the forming operation. The exact-focus images were target-captured for the heated specimens to ensure the achievement of more accurate and reliable results. A load cell consisted of four strain gages in a Wheatstone bridge configuration that was installed above the upper-die assembly to record the peak of the forming load. Figure 4 shows the overall setup of the equipment. The trial performs were produced by electrical discharge machining (EDM) wire cutting. Their faying surfaces were machined and ground by sand paper and then cleaned in acetone and alcohol prior to forge welding. Heat-treated hot work tool steel W302 (equivalent to AISI-H13) was used as the tooling material since this can provide good temper resistance and superior strength under warm-forming conditions. A lubricant with an approximate coefficient of friction of 0.25 was spread over the surfaces of the lower die. After the forming process, the dimensions of the formed components were measured by a digital vernier caliper and a height gage. Some joint interfaces were taken from the selected components, which were inspected by the optical microscope to evaluate the diffusion zone between two dissimilar metals.

RESULTS AND DISCUSSION

All 18 bulk-forming simulations and corresponding experiments with various combinations of T and S were performed. As a satisfactory bimetallic component, a diffusion zone between two dissimilar metals should be able to be found in its joint interface. This was one critical factor among others providing evidence of which of the metals had been cohered properly. Figure 5 shows the micrograph of the bimetallic joint interface obtained from the sample taken in the experimental trial carried out at T = 900°C and S = 40 mm. Three distinct regions were demonstrated. The upper side was the SS316L, the lower side was the AA6063, and the middle was the diffusion zone. The thickness of this diffusion zone was around 4 μm, which was generated in this successful bimetallic component without any macro-defects. The joint of the dissimilar metals was sufficiently reliable that the bimetal would not be broken and separated under the destructive test with the hack saw and files.

Nevertheless, in some simulation and experimental results, the SS316L could not completely fill up the die cavities, in particular the 0.3-mm-thick circular protrusion of the top face of the component. Figure 6 is an example obtained in the process simulated with T = 400°C and S = 20 mm/s. It

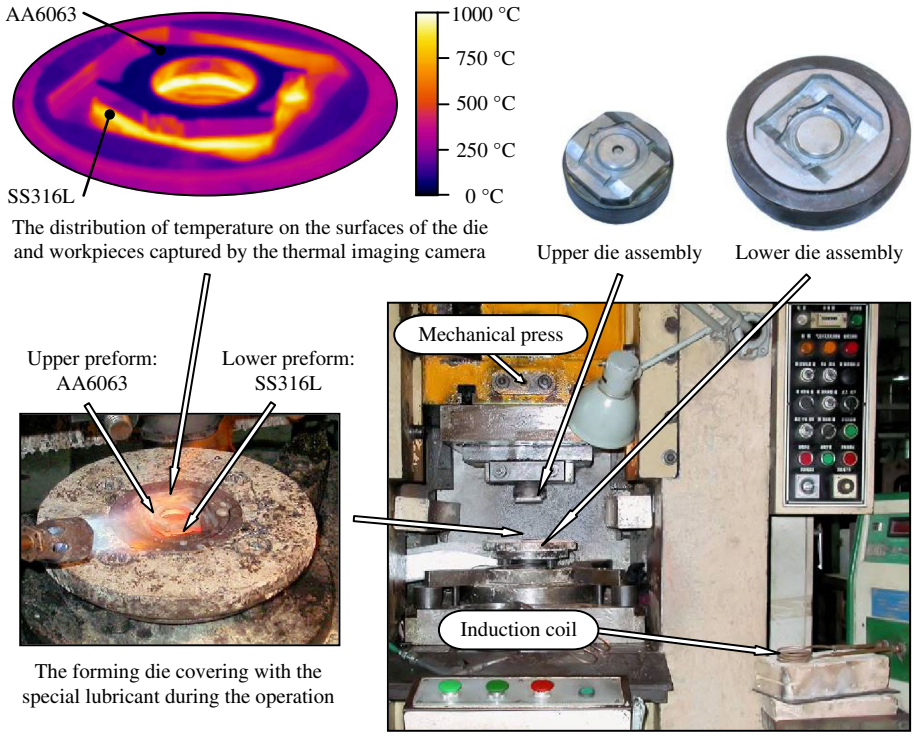

Fig. 4. The experimental setup for bulk forming the component.

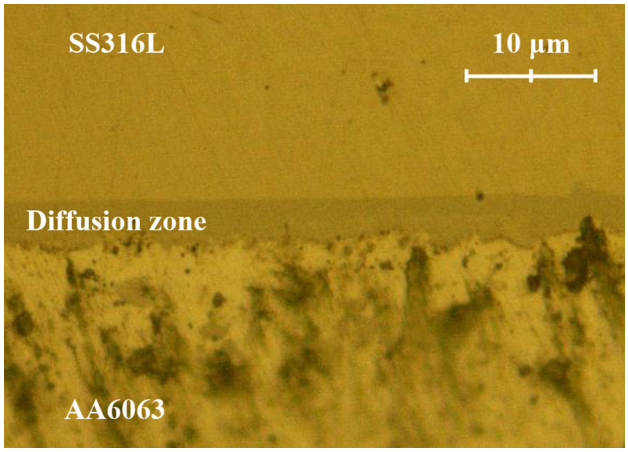

Fig. 5. The micrograph of the bimetallic joint interface shows good cohesion of the sample (T = 900°C and S = 40 mm/s).

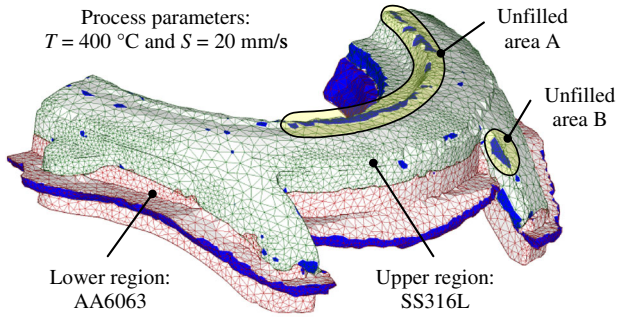

Fig. 6. The unfilled areas of the unsuccessful formed component after simulation.

illustrates that there were two major unfilled areas. The unfilled area A (UA) was located on the top circular protrusion, and the unfilled area B (UB) was near the lateral portion of the lug. These two defects could also be found in most unsuccessful components. Figure 7 shows the completion of die filling in each trial. The y-axis of the graph was labeled the die-filling percentage, which was based on the ratio of the minimum height of UA (measured at the end of the forming stroke) to the full height of UA (i.e., 0.3 mm). A lower percentage meant that a larger cavity of the die had not been filled, whereas the complete die filling was achieved to 100% completion. As shown by both simulation results and experimental measurement, the increases of T and S were able to improve the die filling.

Effects of Temperature

The bulk-forming simulations and experiments were carried out under non-isothermal conditions. The initial temperatures of the two separated preforms and the die components were different, as given in Table V. Heat transfer between their contact surfaces occurred during the process. According to the fundamentals of material deformation behavior, changes of temperature of the preforms highly influenced the material flow as well as the die filling, and hence, this had to be discussed. Both SS316L and AA6063 softened when their temperatures were in-

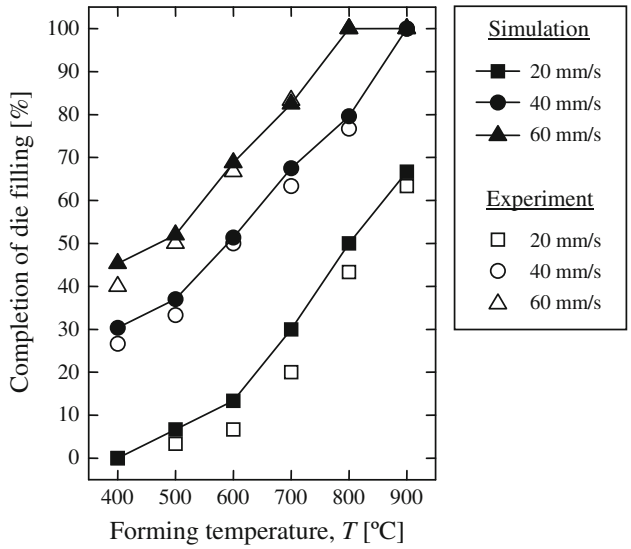

Fig. 7. The completion of die filling for each trial.

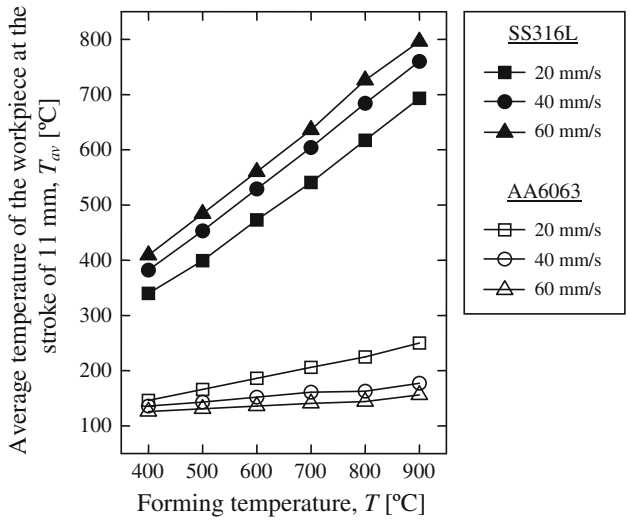

Fig. 8. The simulated average temperatures of SS316L and AA6063 at the stroke of 11 mm for each trial.

creased. Consequently, the temperature discrepancy between these two materials at the identical time step T_{di} should be kept to a certain amount. In other words, the SS316L should be much hotter than the AA6063. This could compensate for the extreme difference of their plasticity so that the die filling is improved considerably. Figure 8 shows the average temperatures T_{av} of SS316L and AA6063 entire workpieces at the stroke of 11 mm (i.e., the end of forming stroke) in each simulation trial. Three trials that achieved the complete die filling were the processes carried out at T = 900°C and S = 40 mm/s, T = 800°C and S = 60 mm/s, and T = 900°C and S = 60 mm/s, their T_{di} being 582°C, 583°C, and 640°C, respectively. On the other hand, the T_{di} of the slightly failed trial (T = 800°C and S = 40 mm/s) was just 521°C. It showed that the T_{di} had a great effect on the die filling in bulk-forming bimetallic components and that the T_{di} higher than 580°C was significant in this present case.

The curves plotted in Fig. 8 were nearly linear within the test range of T, which indicated that the T_{av} drops of SS316L and the T_{av} raises of AA6063 were uniform. The average percentages of T_{av} drops of SS316L for S of 20 mm/s, 40 mm/s, and 60 mm/s were 26.5%, 13.3%, and 6.9%, respectively. When the faster S was used, the T_{av} drops of SS316L were reduced that could increase the T_{di} and get the better die filling. Indeed the T_{av} of SS316L had increased slightly at the forming stroke of around 1 mm since that position was starting deformation of the SS316L and the heat was generated by the compression of material. Therefore, the average percentage of its T_{av} drop was not an exact inverse proportion to the S. On the contrary, the T_{av} of AA6063 was raised much higher at the S of 20 mm/s because the heat from the SS316L could take a longer time to transfer to the AA6063. Since the thermal conductivity of AA6063 was higher than that of SS316L, the degree of change of temperature of AA6063 was larger than that of SS316L.

Effects of Ram Speed

The S not only affected the T_{av} of specimen materials but also extended the effect on material flow. The flow patterns of two different materials during the bulk-forming process were investigated using velocity fields of the simulation. Since the discrepancy of the flow directions was not very noticeable among all 18 trials, the simulation of the processes carried out with the combinations of T of 400°C and 900°C and S of 20 mm/s, 40 mm/s, and 60 mm/s were selected particularly to demonstrate the changing of their velocity fields at the strokes of 10 mm and 11 mm, as shown in Fig. 9. Except for the unfilled areas of the unsuccessful components, the geometries and bimetallic structure of all formed components were similar. Only the influence of S on the magnitudes of velocity was more consequential and had indicated a linear proportional relationship. For instance, the velocities of material flow in the processes taking place at S = 60 mm/s were almost three times those of the processes taking place at 20 mm/s. In considering the material flow at different forming strokes, the materials of the lower region (AA6063) and the materials of the upper region (SS316L) of the components flowed simultaneously at the stroke of 10 mm. However, at the stroke of 10.5 mm, the AA6063 started flowing faster than the SS316L. At the end of the stroke, the SS316L nearly stopped with less deformation and material flow while the AA6063 flowed rapidly. The reason for this was that the flow properties of AA6063 at the initial forming stage were close to those of SS316L; hence, the heterogeneous material flow was minimized and both materials could flow together with parallel velocity fields. Due to the

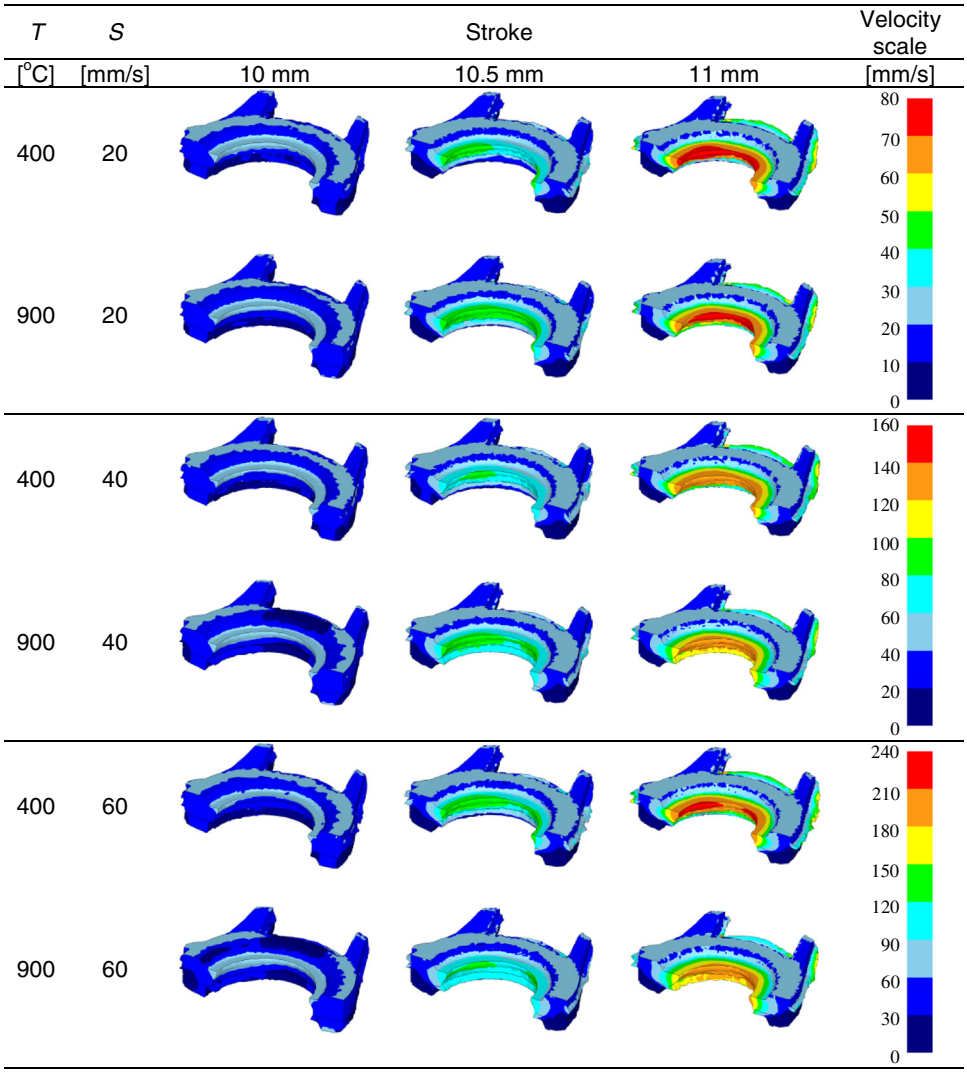

Fig. 9. The simulated velocity field at the stroke of 10 mm, 10.5 mm, and 11 mm for the trials of the process carried out at the combinations of forming temperature (400°C and 900°C) and ram speed (20 mm/s, 40 mm/s, and 60 mm/s), respectively.

rapid increasing of T_{av} of AA6063, from the stroke of around 11.5 mm, the AA6063 became softer than the SS316L such that the material flow mainly occurred in the region of AA6063. Therefore, in bulk-forming SS316L/AA6063 components, particularly at the lower S (i.e., equal or below 20 mm/s), the T must be sufficient or higher (i.e., over 900°C) to lead the completed die filling in the region of SS316L before the softening of AA6063.

The forming load F required for the bulk forming could be predicted by the simulation software as well as recorded in the experiments. Figure 10 shows the peak values of the F in each trial. There was a relatively larger error between simulations and experiments at 400°C and 500°C, which might have been caused by the uncertainties of extrapolation of the missed 500°C flow stress data of SS316L by the simulation software. This 3.7–4.4% error was acceptable since the main purpose of this graph was to reflect the natural phenomenon of T and S to F. The F was influenced significantly by T and S. The F was reduced overall when the T was increased. Although the T_{av} drop of SS316L at the S of 20 mm/s was larger than that at 60 mm/s, the F was higher at the faster S. Consequently, the impact of S on F was more considerable than that of T on F. As die life increased with decreasing F, if the T could be increased, it was recommended to reduce the S of the machine for bulk forming the SS316L/AA6063 components.

Verification by Experiments

To verify the proposed methodology and the results obtained from the computer simulation, physical experiments were conducted using the tailor-made die and a mechanical press specially modified for bimetal bulk forming. The process

conditions were controlled to nearly match the setting of the simulation, with only the T having possible variations of plus/minus 15°C and the S was adjusted as around 20 mm/s, 40 mm/s, and 60 mm/s within the range of forming load. The bimetallic component obtained by the process with T = 900°C and S = 40 mm/s was selected as the most successful example because it was able to completely fill up the die cavity with a minimum F; the peaks of F of this trial in simulation and experiment were 126 ton and 124 ton, respectively. On the other hand, the unsuccessful example was taken from the process with T = 400°C and S = 40 mm/s. These two examples of bimetallic components produced by bulk forming are presented in Fig. 11. Almost no major forming defect was found on the successful formed component, and the accuracy of critical dimensions such as the total width, length, height, and flash thickness was within a tolerance of ±0.08 mm. For the unsuccessful component, the unfilled areas were located nearly the same as the simulation result. Those shapes were close to the results acquired in the simulation that thus confirmed the accuracy and reliability of the software.

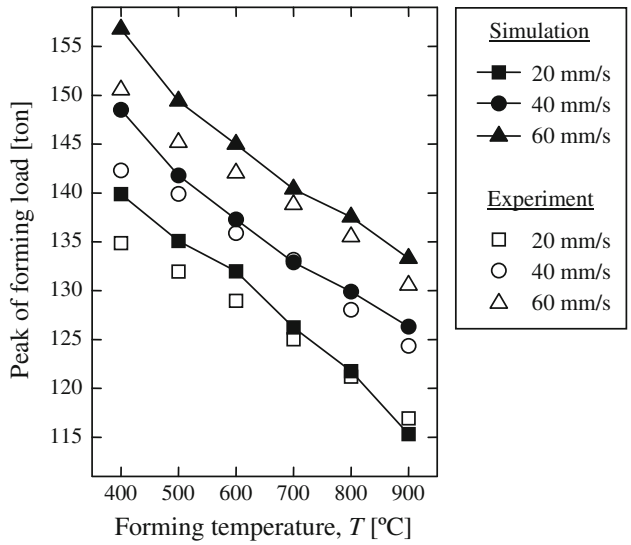

Fig. 10. The forming loads required for forming the components.

CONCLUSION

The material flow in bulk-forming bimetallic SS316L/AA6063 non-axisymmetric watchcase components at forming temperatures T of 400°C, 500°C, 600°C, 700°C, 800°C, and 900°C and ram speeds of 20 mm/s, 40 mm/s, and 60 mm/s has been investigated successfully using the FE simulation. The results showed that the increases of T and S were able to improve the die filling. Since the average temperature T_{av} of AA6063 was increasing during the process, the AA6063 flowed faster than the SS316L. A higher T was thus recommended to avoid the incomplete die filling in the region of SS316L. When the S was increased, a higher forming load F was required to obtain the same plastic deformation. If the T could be increased, a reduction of S was suggested that could save the forming energy and prevent the damage of tooling. Therefore, the most suitable process parameters were T = 900°C and S = 40 mm/s. The experiments were conducted under compatible process conditions to verify the simulation results eventually. The data and the shapes acquired from the experiments, on average, strongly agreed with those predicted by the simulations. This study has demonstrated rationally the success of material-flow prediction for bulk-forming bimetallic components at elevated temperatures, and it has been able to provide a key reference for determining suitable process parameters in such forming processes.

ACKNOWLEDGEMENTS

The work described in this article was supported by Grants from the Research Grant Council of the Hong Kong Special Administrative Region, China (Project No. PolyU 511511).

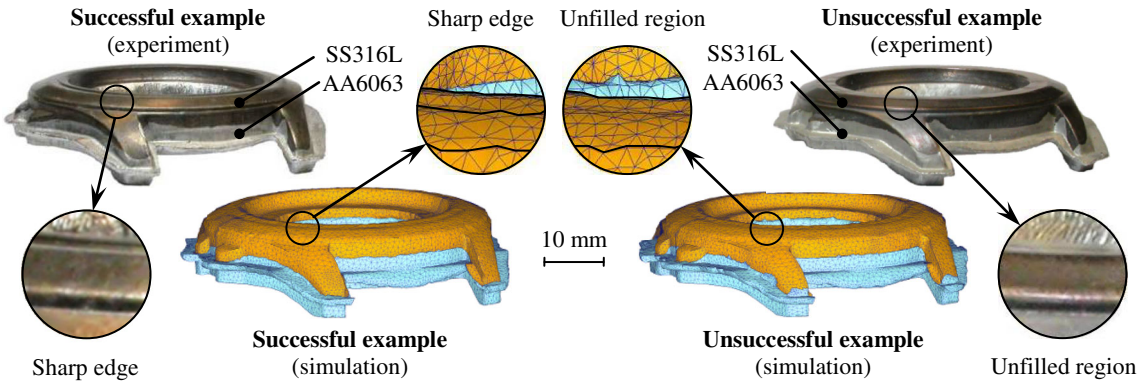

Fig. 11. Comparison of component shapes between simulation and experiment for T = 400°C and 900°C, and S = 40 mm/s.

REFERENCES

1. P. Groche and D. Fritsche, *Int. J. Mach. Tool. Manuf.* 46, 1261 (2006).
2. P. Groche, D. Fritsche, E.A. Tekkaya, J.M. Allwood, G. Hirt, and R. Neugebauer, *CIRP Ann-Manuf. Technol.* 56, 635 (2007).
3. B.A. Behrens, E. Doege, S. Reinsch, K. Telkamp, H. Daehndel, and A. Specker, *J. Mater. Process. Tech.* 185, 139 (2007).
4. S.Z. Sapozhnikov, L.A. Perezhogin, and V.N. Kipriyanov, *Met. Sci. Heat Treat.* 24, 734 (1982).
5. D. Taylor and J. Pan, *Int. J. Mater. Prod. Tech.* 16, 430 (2001).
6. O. Yilmaz and H. Çelik, *J. Mater. Process. Tech.* 141, 67 (2003).
7. M. Şimşir, L.C. Kumruoğlu, and A. Özer, *Mater. Des.* 30, 264 (2009).
8. A.M. Torbati, R.M. Miranda, L. Quintino, S. Williams, and D. Yapp, *J. Mater. Process. Tech.* 211, 1112 (2011).
9. S. Yildirim and M.H. Kelestemur, *Mater. Lett.* 59, 1134 (2005).
10. K.K. Zhang, Y.L. Wang, H.X. Shi, H. Yu, and S. Liu, *Mater. Sci. Eng. A* 499, 97 (2009).
11. N. Kahraman, B. Gülenç, and F. Findik, *J. Mater. Process. Tech.* 169, 127 (2005).
12. S.A.A. Akbari Mousavi and P. Farhadi Sartangi, *Mater. Des.* 30, 459 (2009).
13. T. Altan, S.I. Oh, and H.L. Gegel, *Metal Forming: Fundamentals and Applications* (Materials Park, OH: ASM, 1983).
14. R. Neugebauer, K.D. Bouzakis, B. Denkena, F. Klocke, A. Sterzing, A.E. Tekkaya, and R. Wertheim, *CIRP Ann-Manuf. Technol.* 60, 627 (2011).
15. K. Osakada, K.K. Morib, T. Altan, and P. Groched, *CIRP Ann-Manuf. Technol.* 60, 651 (2011).
16. P. Groche, J. Stahlmann, J. Hartel, and M. Köhler, *Tribol. Int.* 42, 1173 (2009).
17. L. Manuel, J. Stahlmann, and P. Groche (Paper presented at Metal Forming 2012. *Proceedings of 14th International Conference on Metal Forming 2012*, Kraków, Poland, 2012).
18. A. Ahmad, and P. Groche, (Paper presented at NUMIFORM. *Proceedings of 10th International Conference on Numerical Methods in Industrial Forming Processes*, Pohang, Republic of Korea, 2010).
19. S. Berski, H. Dyja, G. Banaszek, and M. Janik, *J. Mater. Process. Tech.* 153–154, 583 (2004).
20. S. Berski, H. Dyja, A. Maranda, J. Nowaczewski, and G. Banaszek, *J. Mater. Process. Tech.* 177, 582 (2006).
21. S. Wohletz, M. Özel, and P. Groche, (Paper presented at New Developments in Forging Technology. *Proceedings of International Conference on New Developments in Forging Technology*, Stuttgart, 2013).
22. N.R. Chitkara and A. Aleem, *Int. J. Mech. Sci.* 43, 2833 (2001).
23. N.R. Chitkara and A. Aleem, *Int. J. Mech. Sci.* 43, 2857 (2001).
24. B.V. Krishna, P. Venugopal, and K. Prasad Rao, *Mater. Sci. Eng. A.* 407, 77 (2005).
25. I.J. Beyerlein, N.A. Mara, J. Wang, J.S. Carpenter, S.J. Zheng, W.Z. Han, R.F. Zhang, K. Kang, T. Nizolek, and T.M. Pollock, *JOM* 64, 1192 (2012).
26. C.A. Bronkhorst, J.R. Mayeur, I.J. Beyerlein, H.M. Mourad, B.L. Hansen, N.A. Mara, J.S. Carpenter, R.J. Mccabe, and S.D. Sintay, *JOM* 65, 431 (2013).
27. S. Raßbach and W. Lehnert, *Comput. Mater. Sci.* 19, 298 (2000).
28. T.F. Kong, L.C. Chan, and T.C. Lee, *J. Mater. Process. Tech.* 167, 472 (2005).
29. S.K. Mannam, V. Seetharman, and V.S. Raghunathan, *Mater. Sci. Eng.* 60, 79 (1983).
30. S. Sundaresan and K.G.K. Murti, *Int. J. Joining. Mater.* 5, 66 (1993).
31. C.M. Chen and R. Kovacevic, *Int. J. Mach. Tool. Manuf.* 44, 1205 (2004).
32. K. Bhanumurthy, R.K. Fotedar, D. Joyson, G.B. Kale, A.L. Pappachan, A.K. Grover, and J. Krishnan, *Mater. Sci. Tech. Lond.* 22, 321 (2006).
33. H. Suzuki, S. Hashizume, Y. Yabuki, Y. Ichihara, and S. Nakajima, *Studies on the Flow Stress of Metals and Alloys* (Tokyo: The Institute of Industrial Science, University of Tokyo, 1986).
34. Y.V.R.K. Prasad and S. Sasidhara, *Hot Working Guide: A Compendium of Processing Maps* (Materials Park, OH: ASM, 1997).
35. J. Fluhrer, *DEFORM-3D Version 6.1 User's Manual*, (Columbus, OH: Scientific Forming Technologies Corporation, 2007).
36. F. Cverna, ed., *ASM Ready Reference—Thermal Properties of Metals* (Materials Park, OH: ASM, 2002).